the considerably more expensive DNMR 3^{17} in selected three- and four-site examples; no difference in the simulated curves was found.

Acknowledgments. We thank the National Science Foundation for financial support of this work, both through Research Grant GP 18844 and the Major Instrument Program. We thank Drs. D. H. Hillenbrand and G. R. Weisman for assistance with NMR data aquisition and processing, and Mr. W. Ehrhardt for use of his program.

References and Notes

(1) For a good review of hydrazine conformational analysis up to 1973, see Y. Shvo, "The Chemistry of the Hydrazo, Azo, and Azoxy Groups", S. Patai, Ed., Wiley, New York, N.Y., 1975, Part 2, pp 1017–1095.
(2) (a) S. F. Nelsen and G. R. Weisman, *J. Am. Chem. Soc.*, **96**, 7111 (1974); (b) S. F. Nelsen and G. R. Weisman, *ibid.*, **98**, 3281 (1976); (c) S. F. Nelsen, *Acc. Chem. Res.*, 11, 14 (1978).
(3) J. E. Anderson, *J. Am. Chem. Soc.*, **91**, 6374 (1969).
(4) G. R. Weisman and S. F. Nelsen, *J. Am. Chem. Soc.*, **98**, 7007 (1976).
(5) (a) S. F. Nelsen, L. Echegoyen, and D. H. Evans, *J. Am. Chem. Soc.*, **97**, 3530 (1975); (b) S. F. Nelsen, L. Echegoyen, E. L. Clennan, D. H. Evans, and D. A. Corrigen, *ibid.*, **99**, 1130 (1977).
(6) (a) J. T. Gerig and J. D. Roberts, *J. Am. Chem. Soc.*, **88**, 2791 (1966); (b) D. K. Dalling, D. M. Grant, and L. F. Johnson, *ibid.*, **93**, 3678 (1971).
(7) Although the carbons of these compounds are numbered properly in the Experimental Section, we have used a consistent (and hence incorrect!) numbering scheme for compounds **8–13**, in which the vinyl carbons (if present) are $C_{8,9}$ and the methylated carbons $C_{2,5}$, for the purposes of reporting the NMR shifts in the body of the paper. Using the conventional numbering causes confusing changes in the designations of the carbons, which are not desirable for our purposes.
(8) (a) D. K. Dalling and D. M. Grant, *J. Am. Chem. Soc.*, **94**, 5318 (1972); (b) R. Freeman, H. D. W. Hill, and P. Kaptein, *J. Magn. Reson.*, **7**, 327 (1972).
(9) (a) E. L. Eliel, *Chem. Ind. (London)*, 568 (1959); (b) E. L. Eliel and R. J. L. Martin, *J. Am. Chem. Soc.*, **90**, 682, 689 (1968).
(10) S. F. Nelsen and G. R. Weisman, *J. Am. Chem. Soc.*, **98**, 3281 (1976).
(11) F. A. Bovey, E. W. Anderson, F. P. Hood, and R. L. Kornegay, *J. Chem. Phys.*, **40**, 3099 (1964).
(12) A. J. Berlin and F. R. Jensen, *Chem. Ind. (London)*, 998 (1960).
(13) S. F. Nelsen, W. C. Hollinsed, and J. C. Calabrese, *J. Am. Chem. Soc.*, **99**, 4461 (1977).
(14) C. Y. Yang and C. H. Bushweller, *J. Am. Chem. Soc.*, **99**, 313 (1977).
(15) F. A. L. Anet and M. Z. Haq, *J. Am. Chem. Scpoc.*, **97**, 3147 (1965).
(16) L. W. Reeves and K. N. Shaw, *Can. J. Chem.*, **48**, 3641 (1970).
(17) D. A. Kleier and C. Binsch, *J. Magn. Reson.*, **3**, 146 (1970).

Low-Temperature Cyclic Voltammetry. 3. Quantitative Comparison of Cyclic Voltammetry and Nuclear Magnetic Resonance as Methods for Conformational Equilibrium and Rate Constant Measurements

Stephen F. Nelsen,* Edward L. Clennan, and Dennis H. Evans

Contribution from the Department of Chemistry, University of Wisconsin, Madison, Wisconsin 53706. *Received September 23, 1977*

Abstract: Low-temperature CV measurements of equilibrium and rate constants for conformational change in 1,6-diazabicyclo[4.4.0]dec-3-ene, its cis and trans 7,10-dimethyl derivatives, and their saturated analogues, the *N,N'*-dimethyl and diethyl derivatives of 3,4-diazabicyclo[4.4.0]decane, 1-ethyl-2-methylhexahydropyridazine, 1,2-diethylhexahydropyridazine, and 2-methyl-1,2-diazabicyclo[4.4.0]decane, are reported. A comparison is made with NMR conformational results for these compounds.

In previous work,[1] it has been established that several six-membered ring hydrazines show a kinetic resolution of the oxidation peaks for conformations with axial, equatorial alkyl groups (Hae, shown below for 1,2-dimethylhexahydropyridazine, **1**) from those with diequatorial groups (Hee, below)

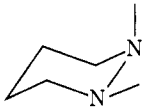

Hae

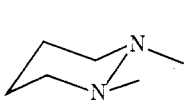

Hee

in cyclic voltammetry (CV) experiments. The oxidation of Hae is slow and electrochemically irreversible while that of Hee is more rapid and nearly reversible. Digital simulations of kinetic Scheme I gave good fit to the observed CV curves.[1b,c] In this scheme the electrode merely samples the concentrations of Hee and Hae, and the conformational change takes place in solution, entirely unaffected by the presence of the electrode. The digital simulations give a value for a kinetic parameter $K_{eq}\cdot\sqrt{k_t}$, where K_{eq} = [Hee]/[Hae], and $k_t = k_{ee \rightarrow ae} + k_{ae \rightarrow ee}$. The values of the kinetic parameters obtained for **2–4** were consistent with ^{13}C NMR derived conformational data,[1b,c]

Scheme I

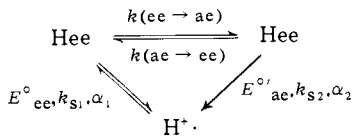

suggesting that Scheme I is a useful picture of what is happening, and that CV can be useful for conformational analysis.

Several factors combined to make our work on **2–4** less than

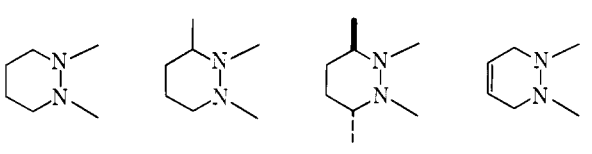

1 2 3 4

a quantitative comparison of the CV and NMR methods for conformational analysis of these compounds. The low temperatures necessary to observe the second (Hae) oxidation peak required the use of butyronitrile (not suitable for NMR work)

0002-7863/78/1500-4012$01.00/0

as solvent. Furthermore, it proved impossible to accurately measure K_{eq} for **2–4** by NMR,[3] so that the CV kinetic parameter expected could not be quantitatively established.

We have extended our CV studies to several systems chosen to allow direct comparison of rate and equilibrium constants derived by NMR (reported separately[4]) with those obtained by CV. The bicyclic hydrazines **5–10** were chosen for this study

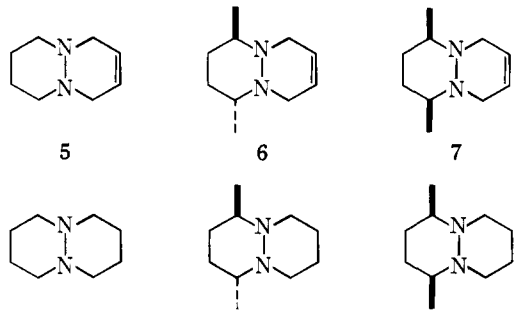

5 **6** **7**

8 **9** **10**

since they have relatively high Hee,Hae barriers (>13 kcal/mol) because of the necessity of coupling ring reversal and nitrogen inversion to convert one conformation to another. This allows low enough temperatures to be reached in acetonitrile (a suitable NMR solvent) to allow measurement of K_{eq} by the CV method. The series covers a wide range of K_{eq} values, varying from too large to measure by NMR (**10**) to too small (**7**).[4] Other compounds for which low-temperature CV data are reported here include the symmetrical diazadecalins **11** and **12**, which also have relatively high ee,ae barriers, and the lower barrier ethylated monocyclic compounds **13** and **14**. The NMR data for **11–14** have been previously discussed.[3-5] Both NMR and CV data for the unsymmetrical diazadecalin **15** are also included.

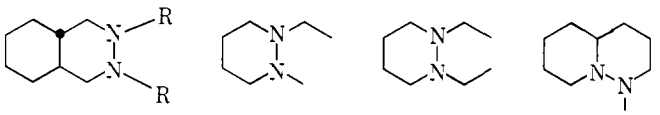

11, R = CH_3
12, R = C_2H_5 **13** **14** **15**

Low-Temperature CV Data for 5–14. A. Digital Simulation Parameters. The apparatus used and techniques employed were like those in our previous work.[1b] Scans were typically recorded at 100, 200, and 500 mV/s using an *X-Y* recorder, and at 1000, 2000, 5000, and 10 000 mV/s on an oscilloscope, at several temperatures where two oxidation peaks could be observed. Only for **8**, which is known to be very predominantly in the ee conformation from NMR work, was no second oxidation ever observed; neither CV nor NMR can give any rate information for such a case. The CV curves obtained were then simulated, using the normal digital simulation technique (see Experimental Section) (when $K_{eq} > 0.1$), or the heterogeneous equivalent method.[1b] The latter is useful when K_{eq} is very low and the rate constants are large because the time required for normal digital simulation escalates.

The curve fitting was done visually, and is not without problems. The most serious problem affecting the accuracy of the conformational data obtained from CV curves is the fact that extra current, not caused by oxidation of Hae and not present in blanks lacking the hydrazine, is observed at the high potential end of the scans. By operating at room temperature with hydrazines which interconvert conformations rapidly, we have found that the irreversible oxidation of $H^{+}\cdot$ to H^{2+} is beginning to contribute to the currents measured for Hae oxidation. At low temperatures and fast scan rates, where the Hae wave moves to higher potential, the interference becomes more serious. The $H^{+}\cdot$,H^{2+} oxidation wave is very broad and irreversible because of the short H^{2+} lifetimes for the compounds considered here, and we have not been able to properly correct for this extra current. It results in the tailing upward at more positive potentials in the experimental curves shown in Figures 1 and 2. The reduction scan shows a single peak, which is smaller than that calculated as can also be seen in Figures 1 and 2. The difference is exaggerated at low scan rates. Since we know from ESR studies that $H^{+}\cdot$ does not decompose appreciably in the absence of the electrode on the CV time scale (at least at the lower temperatures employed), the loss of $H^{+}\cdot$ is presumably caused by the presence of the electrode but the precise cause of the diminution of the reduction peak is unknown. We have not seriously tried to account quantitatively for this loss of current in the reduction scan; only the oxidation scan is used for extraction of conformational information in this phase of our work anyway.

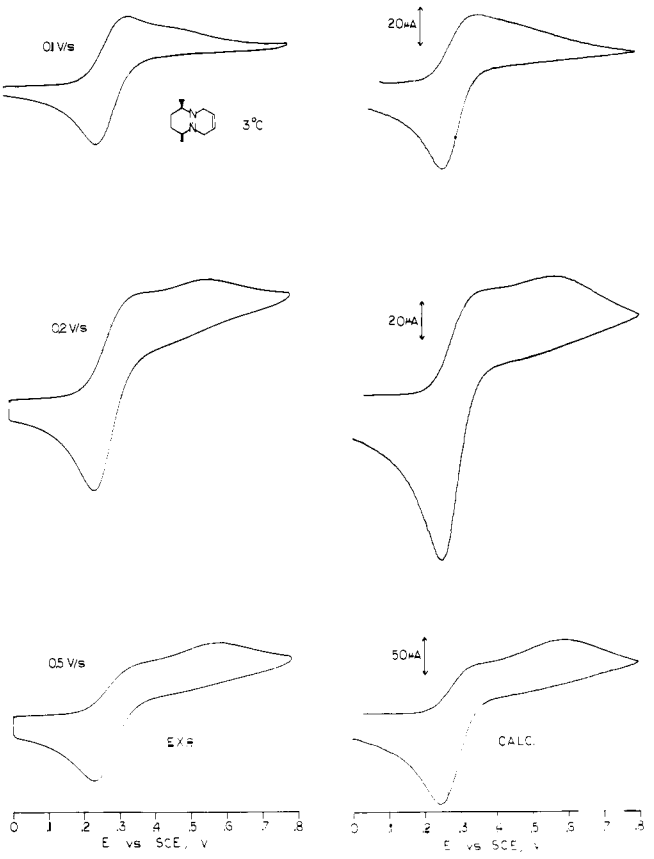

Figure 1. Slow-scan (recorder traced) CV curves for **6**, at 3 °C, compared with simulated curves. Potential increases to the right, and positive current is up, in contrast to the usual electrochemical convention.

Typical CV curves and simulated curves are shown in Figures 1 and 2. Although several parameters are needed to fit the curves,[1b] the conformationally important ones are the kinetic parameter, $K_{eq}\sqrt{k_t}$, and α_2, which appear in Table I. A value for K_{eq} must be assumed to obtain the kinetic parameter when K_{eq} is above about 0.03, and the values used are discussed below. The value of α_2 used was that necessary to get the proper broadening and E_p shift with scan rate for the Hae peak. The effect of changing α_2 on $K_{eq}\sqrt{k_t}$ is illustrated by data sets 22 and 23, where values of 0.45 and 0.50, which gave simulations we deemed equivalent, yielded $K_{eq}\sqrt{k_t}$ values differing by 14% at −13 °C, and less at −23 °C. Use of α_2 values of 0.40 or 0.55 gave simulations which deviated more from the experimental data. We note that the α_2 values required for best fit of the data did not change with temperature, except in data sets 8–11. These were the only experiments run without *iR* compensation, which causes increasing distortion of the data as the temperatures is decreased and the scan rate increased.

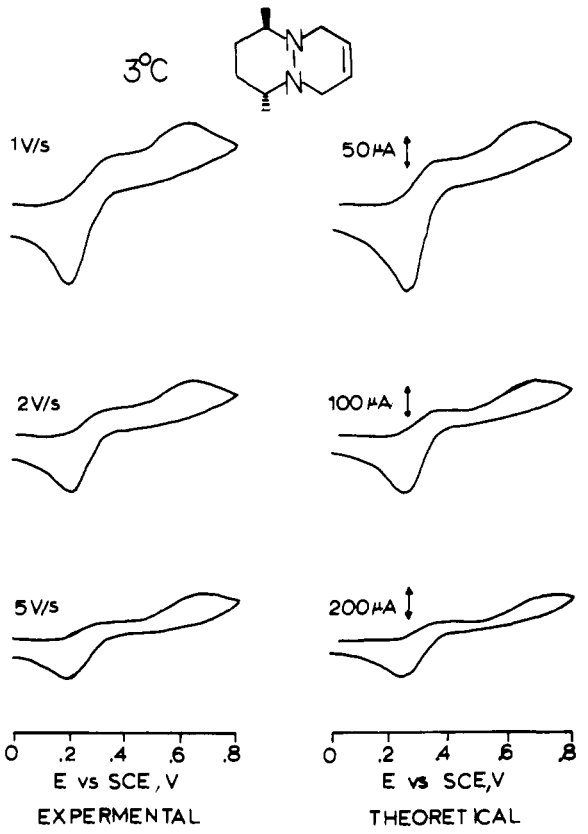

Figure 2. Fast-scan (oscilloscope traced) CV curves for **6**, at 3 °C, compared with simulated curves.

The reproducibility of the kinetic parameter obtained is shown graphically in Figure 3, where the data for **6** are plotted. Most of the points fall within about 10% in $K_{eq}\sqrt{k_t}$ of a line through the data points. The data which were not *iR* compensated seem to deviate noticeably at lower temperatures, where the solution *iR* drops are larger. All other data employed *iR* compensation. Data for **7** were determined in all three solvents employed in this work, with little apparent effect on the kinetic parameter, as expected from NMR experiments.

B. Equilibrium Constants. Comparison with NMR Data. At low enough temperature and fast enough scan rate, the relative sizes of the Hee and Hae oxidation peaks no longer are scan rate dependent; the ee,ae equilibrium has then been "frozen out" on the CV time scale. Under these conditions, the digital simulations yield K_{eq} values. Table II contains the data sets where K_{eq} was obtained by CV in this manner. The temperatures necessary to achieve K_{eq} measurement are generally those at which great broadening is observed by ^{13}C NMR. Also included in Table II are K_{eq} values obtained by NMR in the same solvent for comparison with the CV data. The NMR values represent interpolations of higher and lower temperature data.[4] It will be noted that relatively good agreement between the two types of measurement was found, but also that the CV-derived K_{eq} values are systematically slightly lower than the NMR values. This is consistent with the interference from oxidation to the dication noted above. A contribution from the second oxidation process will make the Hae peak "too large" relative to the Hee peak, and lower the K_{eq} value calculated. The size of the CV underestimation of K_{eq} will depend upon K_{eq}, because a small error in the Hae current will be more important if this current is small (that is, if K_{eq} is large). We note that $\Delta\Delta G°$ is largest for **5**, which has the largest K_{eq} value.

We believe that the differences in K_{eq} as evaluated by CV and NMR are encouragingly small, especially when the 100–1000-fold difference in hydrazine concentration between the two experiments is considered. The CV experiment was performed in the presence of 0.1 M supporting electrolyte, tetrabutylammonium perchlorate, but we found that addition of 0.1 M concentration of supporting electrolyte to a 0.9 M solution of **6** did not affect the K_{eq} obtained by NMR detectably. Although we cannot achieve the 10–100-fold excess of supporting electrolyte present in the CV experiment to really investigate a small drift in the NMR-derived K_{eq} value, there is no evidence that the presence of supporting electrolyte affects K_{eq} appreciably.

C. Rate Constants. Comparison with NMR Data. Rate constants for conformational change obtained by CV experiments were calculated from the kinetic parameters in Table I, using the CV K_{eq} values from Table II. At higher temperatures, where K_{eq} was not directly measured by CV, the value of K_{eq} employed was estimated from the lower temperature CV value by employing $\Delta S° = 0$, which we know from the NMR work to be a good assumption for these compounds.

The NMR-derived rate constants in Table III were calculated from the data of ref 3 and 4. Because the lifetime of a carbon in one magnetic environment for an Hae conformation is affected by both the coupled nitrogen inversion and ring reversal (abbreviated N,R) which converts Hae to Hee, and also by double ring reversal (R,R) which converts ae to ea, the NMR experiment has a tendency to confuse these processes. The higher k(ae → ee) value, or the only one, was calculated

Table I. Kinetic Parameters Derived from Digital Simulations of CV Curves for Some Diazadecalins

Compd	Data set	Temp, °C	Solvent	α_2	$K_{eq}\sqrt{k_t}$
5	1	−5	Acetone	0.3	12.8
	2	−15	Acetone	0.3	10.1
	3	−25	Acetone	0.3	8.1
6	4	22	Acetonitrile	0.3	4.2
	5	−10	Acetonitrile	0.3	0.46
	6	−23	Acetonitrile	0.3	0.13
	7[a]	21	Acetonitrile	0.3	3.6
	8[a]	7	Acetonitrile	0.3	1.4
	9[a]	−12	Acetonitrile	0.5	0.64
	10[a]	−24	Acetonitrile	0.4	0.16
	11	15	Acetonitrile	0.3	2.1
	12	3	Acetonitrile	0.3	1.0
	13	−22	Acetonitrile	0.3	0.13
7	14[b]	24	Butyronitrile	0.3	2.2
	15[b]	4	Butyronitrile	0.3	0.76
	16[b]	−12	Butyronitrile	0.3	0.23
	17[b]	23	Acetonitrile	0.3	2.1
	18[b]	6	Acetonitrile	0.3	0.70
	19[b]	−10	Acetonitrile	0.3	0.23
	20[b]	19	Acetone	0.3	1.9
9	21	0	Acetonitrile	0.45	12.6
	22	−13	Acetonitrile	0.45	6.8
				[0.5]	[7.9]
	23	−23	Acetonitrile	0.45	3.2
				[0.5]	[3.2]
10	24	14	Acetonitrile	0.4	20.0
	25	−2	Acetonitrile	0.4	9.3
	26	−15	Acetonitrile	0.4	3.6
	27	−27	Acetonitrile	0.4	1.5
11	28	−38	Acetone	0.3	4.0
12	29	−18	Acetone	0.4	2.7
	30	−2	Acetone	0.4	0.94
14	31	−67	Acetone	0.3	1.8
15	32	−39	Acetone	0.3	1.0
	33	−55	Acetone	0.3	0.53

[a] These data not *iR* compensated. All others were. [b] Heterogeneous equivalent program employed. Direct simulations take prohibitively long when K_{eq} is small, and rate constants are large as they are for this compound at high temperature.

Table II. Comparison of CV and ^{13}C NMR Derived Equilibrium Constants

Compd	Data set	Temp, °C	K_{eq} (CV)	K_{eq} (NMR)[a]	$\Delta\Delta G°$, kcal/mol[b]
5	2	−15	1.9	3.8	+0.36
	3	−25	2.2	4.1	+0.30
6	5	−10	0.17	0.21	+0.11
	6	−23	0.15	0.19	+0.12
	13	−22	0.15	0.19	+0.12
7	16	−12	*c*	*c*	
	19	−10	*c*	*c*	
9	23	−23	1.4,[d] 1.3[e]	1.8	+0.17,[d] 0.13[e]
10	27	−27	0.56	0.98	+0.27
11	28	−38	1.1	1.3	+0.10
12	30	−2	*c*	*c*	

[a] See ref 4. [b] $\Delta G°$ (CV) − $\Delta G°$ (NMR) at temperature employed. [c] Too small to measure ("all Hae"). [d] Calculated with $\alpha_2 = 0.50$. [e] Calculated with $\alpha_2 = 0.45$.

assuming that the R,R process was negligibly slow compared to the faster N,R process. If R,R actually has a significant rate, a smaller N,R rate constant will fit our data equally well, but a limit may be placed upon the maximum acceptable R,R rate, and hence on the minimum acceptable N,R rate. At some temperatures, it was possible[4] to show that R,R was in fact quite slow, and that only a small range of k(ae → ee) values would fit the NMR data, but we do not have good estimates of the minimum acceptable rate at all temperatures. It may be seen from Table III that the range of NMR rates is in practice quite narrow.

Neither the NMR nor the CV data are of the same quality for all compounds. The quality of the NMR data is strongly affected both by the number of accidental overlaps which occur as the peaks broaden, and hence upon the number of magnetically different carbons and by $\Delta\delta$ for carbons which are resolved. Both factors are unimportant for the CV data. Even with only four peaks present at high temperature for **4**, two happen to overlap badly, and a third had too small a $\Delta\delta$ for NMR analysis. We were forced to resort to deuteration to have

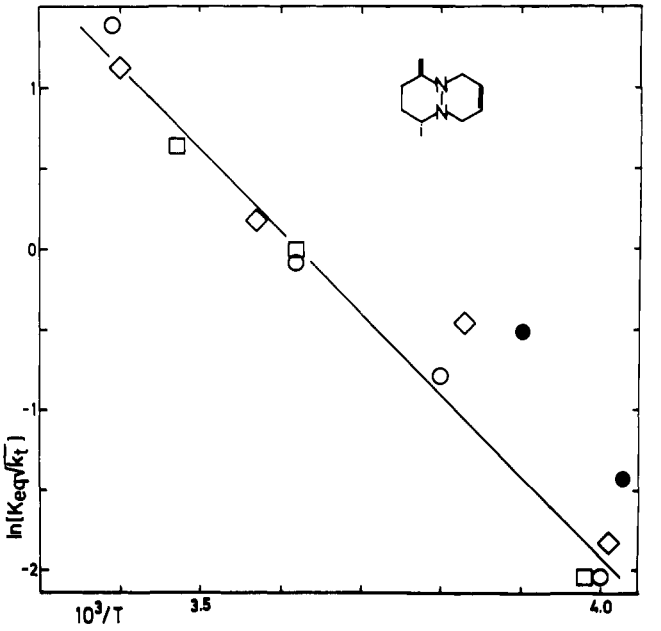

Figure 3. Plot of ln $K_{eq}\sqrt{k_t}$ vs. $10^3/T$ for **6**, illustrating the reproducibility of kinetic parameter measurement by CV. Different symbols represent data sets collected on different days: ○, sets 4-7; ◇, sets 8-11 (no *iR* compensation); □, sets 12-14. The size of the circle represents a 5% variation in the kinetic parameter. The filled circles represent measurements from second oxidation scan data.

even two analyzable types of carbons for NMR analysis of **5**.[4] The NMR spectra of **9** are particularly complex, and difficulties with their analysis make the NMR rate constants particularly suspect for this compound; we include these numbers in brackets in Table III.

We believe that the CV data are particularly suspect for **5**, because of its large K_{eq} value. This makes the Hae peak small and hence greatly affected by small contributions from the second oxidation. The K_{eq} values determined by CV for **5** were noticeably in poorer agreement with the NMR values than data for smaller K_{eq} compounds, and we believe that the CV

Table III. Comparison of CV and ^{13}C NMR Rate Constants for Conformational Change

Compd	Data set	Temp, °C	k(ae → ee), CV, s^{-1}	k(ae → ee), NMR,[a] s^{-1}	Ratio NMR/CV k(ae → ee)	Ratio NMR/CV k(ee → ae)
5	1	−5	25	13.5	0.54	0.27
	2	−15	19	3.9	0.21	0.09
	3	−25	9	1.0	0.11	0.05
6	4	22	72	99-118	1.4-1.6	1.1-1.3
	5	−10	1.1	3.3-4.0	3.1-3.8	2.5-3.1
	6	−23	0.9	0.79	0.8	
	7[b]	21	45	90-107	2.0-2.4	1.8-2.2
	8[b]	7	7.3	22-27	3.0-3.6	2.8-3.4
	9[b]	−12	2.1	3.3	1.6	1.3
	10[b]	−24	0.1	0.67	6.1	5.8
	11	15	19	49-60	2.7-3.2	2.0-2.5
	12	3	5.1	17	3.0	2.7
	13	−22	0.09	0.44	4.7	7.4
9	21	0	53	93-96	1.8-1.8	1.4-1.4
	22	−13	18,[c] 13[d]	25-27	1.3-1.4[c] 1.6-1.7[d]	1.1-1.2[c] 1.2-1.3[d]
	23	−23	3.1,[c] 3.5[d]	8.8	2.9,[c] 2.6[d]	2.3,[c] 1.9[d]
10	24	14	407	[2460][e]	[6.0]	[3.6]
	25	−2	93	[580][e]	[6.3]	[3.5]
	26	−15	15	[160][e]	[11.1]	[5.9]
	27	−27	2.6	[40][e]	[15.0]	[7.5]
11	28	−38	6.7	5.9	0.9	1.0

[a] See text for explanation of the ranges quoted. [b] These data not *iR* compensated; all others were. [c] Calculated using $\alpha = 0.45$. [d] Calculated using $\alpha = 0.50$. [e] Very inaccurate. See text.

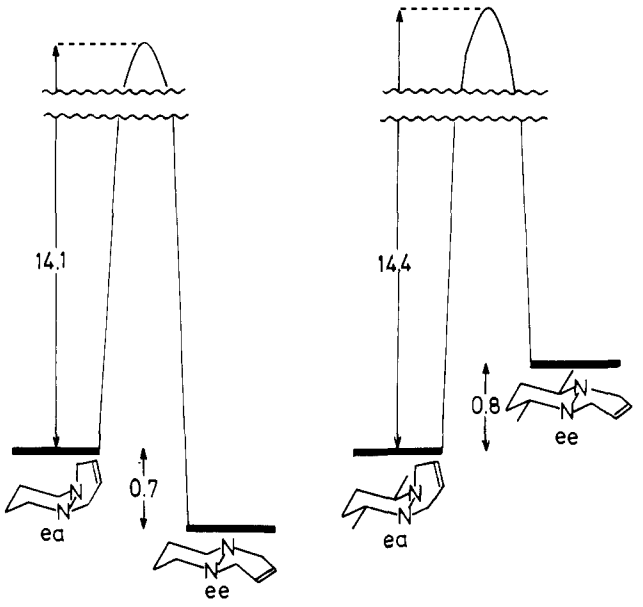

Figure 4. Comparison of NMR-derived barrier heights for **5** and **6**.

rate constants are also most likely to be in error.

The data for **6, 8,** and **11** provide reasonable comparisons of the NMR and CV methods for more favorable cases for CV work. The CV rates are seen to agree at the higher temperatures to within about a factor of 3 with the NMR numbers. The CV rate constants are not as reproducible as the NMR rates, and are based upon less data. At lower temperatures, where the relative size of the Hee and Hae peaks no longer changes with scan rate and K_{eq} can be directly measured, the accuracy of the kinetic parameter that can be estimated suffers, because the scan rate range where changes are occurring necessarily becomes narrower. We believe that this is the principal reason for the greater scatter of the low-temperature CV rate constants (compare data sets 6, 10, and 13).

We believe that the agreement between the NMR- and CV-derived rate constants for **6, 8,** and **11** is quite encouraging. The CV rate data are probably to be preferred for **9,** which has difficulties for NMR analysis.[4]

D. Combining CV and NMR Data. We are more confident about being able to combine the data derived from CV and NMR experiments to yield extra information now that it is apparent that both rate and equilibrium constants estimated by the two methods are numerically close.

No equilibrium constant is directly available by CV or NMR for **7** because so little **7**ee is present under "frozen-out" conditions that peaks for this conformation are not detectable. The kinetic parameter (see Table I) is as easily measurable for **7** as for compounds with higher K_{eq} values. If rate constants can be estimated, the kinetic parameter should allow estimation of K_{eq} for **7**. As is shown diagrammatically in Figure 4, NMR $\Delta G^{\ddagger}$ (ae → ee) values for **5** and **6** are similar, so the rate of this N,R process has been shown to be rather insensitive to the effect of methylation. The slightly higher $\Delta G^{\ddagger}$ obtained for the trans dimethyl compound, **6,** may reflect part of the destabilization of **6**ee relative to **6**ae appearing in the transition state for its formation. We therefore estimate $\Delta G^{\ddagger}$ (ae → ee) for **7** to be most likely in the range 14.25–14.75 kcal/mol. Because $\Delta G°$ is large, k_t in the kinetic parameter is completely dominated by k (ee → ae), so rates for this process which give $\Delta G^{\ddagger}$ (ae → ee) in the range quoted were devised, giving $\Delta G°$ (24 °C) = 2.0 ± 0.25 kcal/mol when $\Delta G^{\ddagger}$ (ae → ee) = 14.5 ± 0.25, $\Delta G^{\ddagger}$ (ee → ae) = 12.5 ± 0.5. The 4 and −12 °C kinetic parameters were also consistent with these figures. The NMR data allow a crude estimate of $\Delta G°$ as being greater than about 1.5 kcal/mol (or else **6**ee should have been detected). The CV kinetic parameter observed makes it unlikely that K_{eq} is higher than about 2.2 or lower than about 1.7, or the $\Delta G^{\ddagger}$ (ae → ee) required would be incompatible with those for analogous compounds.

Table IV. Comparison of NMR and CV Derived Rate Constants for **14** at −67 °C in Acetone

	NMR[a]	CV[b]
k(ee → ae)	315	341
k(ae → ee)	37.6	31

[a] From ref 1. [b] Calculated using K_{eq} = 0.092, determined by NMR[3b] at −74 °C.

Although the kinetic parameter for **13** was measured at −67 °C, the Hee,Hae barrier is too low to allow a "frozen" voltammogram to be recorded. Combining the NMR K_{eq} value, measured by integration at −74 °C, with the CV kinetic parameter gives rate constants in excellent agreement with those obtained by NMR,[3b] as shown in Table IV.

The diethyl compound **14** has such a low K_{eq} that it was not measured either by NMR or CV. The highest barrier separating Hae from Hee for this compound is the nonpassing ring reversal barrier.[3b] Since its height is determined by the ease of attaining the half-chair conformation which alters geometry at the nitrogens very little (indeed, this ring reversal barrier is experimentally the same for dimethylhexahydropyridazine as for cyclohexane[3a]), we may confidently expect a 10 kcal/mol $\Delta G^{\ddagger}$ for **14**ae → **14**ee. Combining this with the kinetic parameters of Table I, K_{eq} is estimated to be 0.02 at −39 °C ($\Delta G°$ = 1.8 kcal/mol), and 0.02_5 at −55 °C ($\Delta G°$ = 1.6 kcal/mol). We are pleased with the difference of only 0.2 kcal/mol between the $\Delta G°$ values estimated at these two temperatures. A further check on the size of this equilibrium constant is provided by the kinetic parameter for **12.** We know from NMR work[3a] that **1** and **11** have, as might be expected, K_{eq} values very close to each other; the diethyl analogues **12** and **14** will also have very similar K_{eq} values. Using a value for K_{eq} of **14** of 0.02, one obtains a k(ae → ee) value at −18 °C corresponding to $\Delta G^{\ddagger}$ = 11.6 kcal/mol, a reasonable value for a "passing" nitrogen inversion. The CV and NMR data for **11**–**14** are internally consistent, and agree remarkably well with each other. Combining the data allows a considerably better estimation of the $\Delta G°$ for these compounds than is available from either technique alone.

Conformational Analysis of 15. A. NMR Studies. As shown in the conformational diagram (Figure 5), **15** is a very complex case for study. It has nine different carbons in each of six possible conformations, and there are nine different conformational equilibria connecting these conformations. It was by no means obvious that useful conformational information would result from the NMR study at the outset of this work. The fast exchange spectrum was observed at 69 °C, and all peaks broadened upon lowering the temperature. By −52 °C, the spectrum consists of nine sharp lines (species A) superimposed on a set of eight conformationally broadened lines; one conformation is no longer rapidly interconverting with the others. Further cooling did not change the line widths for species A, but the other lines broadened and then sharpened to a set of eight lines (species B, one carbon probably overlaps with one species A carbon), and a set of very small lines, just visible above baseline noise. The chemical shifts are collected in Table V. Species A was easily assigned as the e(ee) conformation from its chemical shifts.

Using the shifts observed for replacing CH by N in going from diequatorial 1,2-dimethylpiperidine to diequatorial 1,2-dimethylhexahydropyridazine[6] to estimate the expected peak positions for **13**e(ee) from those found for **16**[7] (which is overwhelmingly in the conformation indicated) reproduced

Table V. Chemical Shifts (ppm) for **15**, 2.8 M in Acetone-d_6

Temp, °C Assign- ment	69 Equili- brating	−74 Sp. A, e(ee)	−74[a] Sp. B, e(ea)
C_3	55.24	58.63	52.25
C_4	22.09	24.69	17.21
C_5	31.59	33.01[b]	33.26[b]
C_6	57.17	63.73	54.57
C_7	34.21	33.86[b]	Unobsd
C_8	24.36	25.18	26.59[c]
C_9	26.98	26.51[c]	28.33
C_{10}	50.99	52.57	49.60
Me	37.75	44.44	34.75

[a] Minor conformation peaks discerned at 19.31, 19.92, 23.89, 24.17, 37.09, 41.98, 43.17, 47.14, 56.57 ppm. [b,c] Assignments could well be reversed.

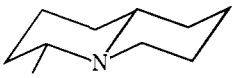

16

the observed spectrum for species A very well (average deviation 0.14 ppm, maximum deviation 0.56 at C_8; see the Experimental Section for the comparison). Species B is also confidently assigned to e(ea) from its chemical shifts. Large upfield shifts occur in species B compared to e(ee) at C_4, C_6, and NMe, all of which gain a 1,3-diaxial interaction when N_2 is inverted, and also at C_3. The respective shifts to lower δ are 7.48, 9.16, 9.86, and 6.38 at the carbons mentioned for species B compared to species A. For ae and ee 1,2-dimethylhexahydropyridazine, shifts of 9.72, 15.25, 18.22, and 4.00 were observed for the corresponding carbons.[6] Although the carbons gaining a 1,3-diaxial interaction are shifted less in the bicyclic than in the monocyclic system, there is a reciprocal change in the size of the C_3 shift. Upfield shifts for axial vs. equatorial *C*-methyl compounds, including 1-methyldecalins[8] and 5-methylquinolizidines,[7] are significantly smaller than in either the mono- or bicyclic hydrazines. Nevertheless, it is clear that the ring fusion is trans in both species A and B, and that they differ by N_2 inversion. It is not surprising that the trans diazadecalins **15**e(ee) and **15**e(ea) dominate the conformation of **15**, because *cis*-decalin is destabilized by 2.7 kcal/mol compared to *trans*-decalin.[9]

Several tiny peaks were also observed in the low-temperature spectra of **15**, and are listed in a footnote of Table V. We are unable to assign the nine peaks reported to either a(ee) or e(ae) based on estimations from the known chemical shifts of the related quinolizidines.[10,11] One problem could be that e(ae) would still be in equilibrium with e(aa) at all temperatures employed, and there could be enough of the diaxial compound to shift the peaks significantly. There is, however, evidence that this is not the only problem. We report no peak near 30-33 ppm, where both a(ee) and e(ae) conformations have a peak. There are many assigned peaks in this region (including the acetone multiplet), and small peaks might very well be unresolved. We suggest that either some impurity peaks have been misidentified, or more than one minor conformation is actually present, and several peaks of each have been unresolved. Although we cannot assign conformations to the small peaks, it is required that at least one cis-fused diazadecalin is responsible for at least some of the small peaks, to account for the broadening of the spectrum between −50 and −70 °C.

To attempt to establish the equilibrium constant, $K_{eq}' = [e(ee)]/[e(ea)] + [minor]$, the methyl carbons were integrated in the temperature range −75 to −89 °C, giving K_{eq}' values of 0.6 ± 0.1. The ratio of e(ea)/minor peak areas was about 85-90:10-15 in this temperature range. An estimate of K_{eq}' at high temperature by the chemical shift interpolation method was accomplished by using temperature extrapolated shifts

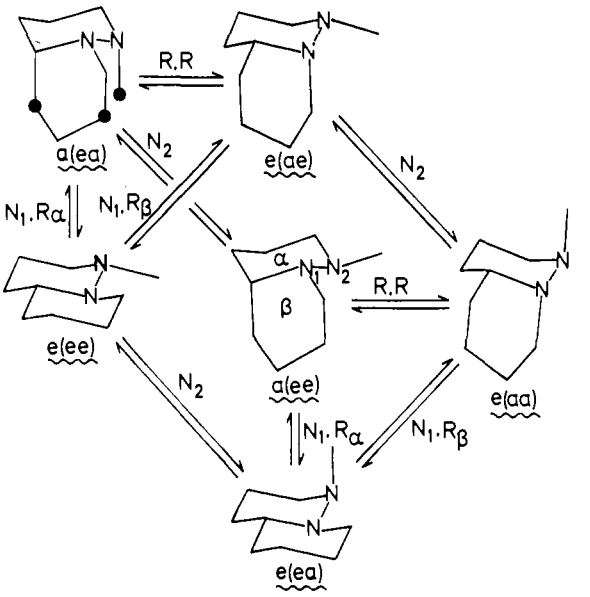

Figure 5. Conformational diagram for **15**.

for e(ee) and the weighted average of e(ea) and minor (holding the mixture at 87:13, which is a poor approximation) for the methyl and C_6 carbons yielded K_{eq}' values in the range 0.33-0.43 between 9 and 69 °C. Comparison of data by the two methods is not very satisfactory (a Van't Hoff plot had a correlation coefficient of only 0.92, and the calculated $\Delta S°$ of −3.3 ± 0.5 is unrealistically low), but we feel that they establish that e(ea) predominates over e(ee). This seems reasonable, because although ee predominates very slightly over ae for 1,2-dimethylhexahydropyridazine and its 4,5 trans-fused decalin analogue **11**, the greater rigidity of the alkyl substituent at N_1 of **15** could well be expected to cause a greater steric interaction in **15**e(ee) than in **11**ee. The activation barrier separating **15**e(ee) from the **15**e(ea)/minor mixture, the first conformational process which affects the NMR spectrum as the temperature is lowered, was estimated by digital simulation in the 9-41 °C temperature range (above T_c for the process), giving $\Delta G^{\ddagger}$ [e(ee) → e(ea)/minor] of 12.4, $\Delta G^{\ddagger}$ [e(ea)/minor → e(ee)] = 13.0 at 25 °C. Such a barrier is quite consistent with that expected for the "passing" N_2 inversion for **15**. It seems logical that the barrier measured does correspond to this passing N_2 inversion, because the other two processes which could convert e(ee) to e(ea), N_1,R_β and N_1,R_α each has a passing ring reversal coupled with nitrogen inversion, which should raise the barriers. The spectra are only consistent, however, with the barriers connecting e(ea) with the minor conformation being lower than (or comparable to—T_c is also affected by $\Delta\delta$) the N_2 inversion barrier. The complexity of the NMR spectrum of **15** makes extraction of conformational information very difficult, and the numbers obtained are unquestionably less reliable than those for more symmetrical systems.

B. CV Studies. Low-temperature CV data were collected for **15** at −30 and −45 °C. An anomaly shown by this compound was that the Hae oxidation peak was unusually broad, and required the alarmingly low α_2 value of 0.16 for successful simulation. One possibility suggested by the NMR work is that two Hae species might actually be present, and if these had significantly different heterogeneous electron transfer rates, the Hae peak would really be a superposition of two peaks with different peak potentials. At −45 °C, a K_{eq} value of 0.22 was measured by CV. This is lower than the K_{eq} values measured by NMR (which we know to be rather inaccurate). The rates obtained by combination of the CV K_{eq} value with the kinetic parameters were very close to the ones obtained by NMR for the e(ee) ⇌ e(ea)/minor processes: k(e(ee) → e(ea)/minor)

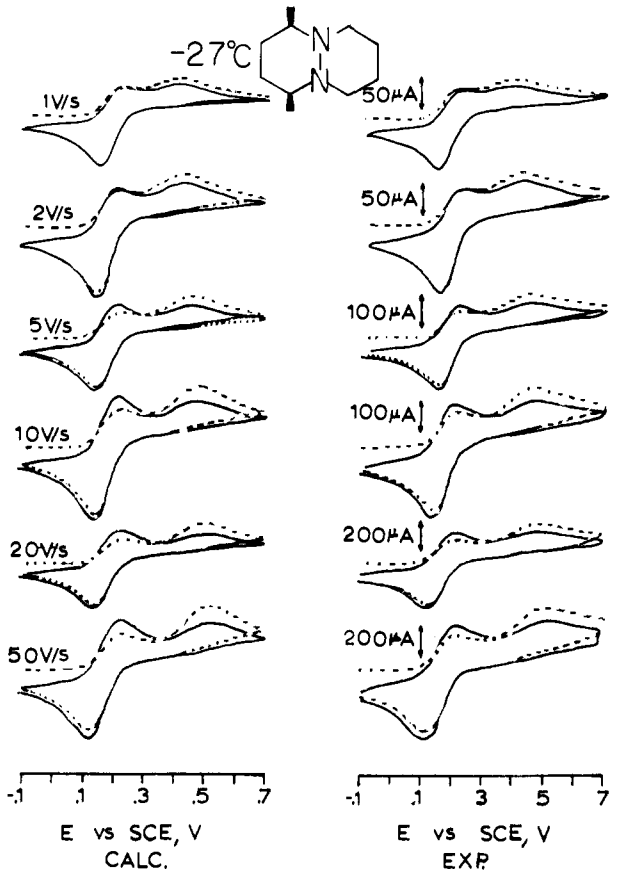

Figure 6. Comparison of calculated and experimental second scan CV curves for 10 at −27 °C. Second scans were calculated using the simulation parameters which fit the first scans. Dotted line is the first scan, solid the second.

NMR/k(ee → ae) CV, 32/33 (−30 °C), 5.7/7 (−45 °C); k(e(ea)/minor → e(ee) NMR/k(ae → ee) CV, 14/8 (−30 °C), 2.7/1.5 (−45 °C). It appears that a rate constant at least close to that measured by NMR for the N_2 inversion is the process which interconverts Hee and Hae for this system. The CV work provides support for our interpretation of the very complex NMR results, and we suspect that the equilibrium constant measured by CV is the more reliable one, which seems most consistent with the minor conformation unassignable by NMR having axial, equatorial alkyl attachment.

C. Second Scan Experiments. Kinetic Scheme I, which has been shown to be kinetically useful, requires that reduction of $H^+\cdot$ gives exclusively Hee, even if Hae is more stable. The easiest way to test this prediction is to run a second scan immediately after the first. If k(ee → ae) is low enough on the time scale of the experiment, the Hee wave will be increased in size relative to that of the first scan. Larger second scan Hee waves than those observed on the first scan have been seen for **6, 7,** and **9**. The second scan may be simulated in the same manner as the first. As shown in Figure 6, such simulations, using parameters which fit the first scan best, also fit the second scan well for **9** at −27 °C. Here, where K_{eq} is near 1, k(ee → ae) and k(ae → ee) are similar, and become slow on the time scale of the experiment in the same temperature range. The good fit to the second scan provides an additional quantitative test of Scheme I. Measurement of $K_{eq}\sqrt{k_t}$ by simulating best fit to the second oxidation scan curve gives a value of 1.9, compared to the 1.5 which gives best fit to the first scan curve.

The second scan experiment is potentially far more useful for cases where K_{eq} is very small. For such a case, k(ee → ae) is much larger than k(ae → ee); although first scan experiments allow measurement of the kinetic parameter, $K_{eq}\sqrt{k_t}$ ($k_t \simeq k$(ee → ae) here because of the rate imbalance), once k(ae → ee) has become slow on the time scale of the experiment, the Hee peak has essentially disappeared from the first oxidation scan, and neither K_{eq} nor the kinetic parameter can be measured. Once k(ae → ee) has become "frozen out", however, the size of the Hee wave on the second scan is controlled only by k(ee → ae), so that this rate may be independently measured by simulation of the second oxidation scan at low temperatures. Measurement of k(ee → ae) allows determination of K_{eq} from the kinetic parameter measured at higher temperatures. The accuracy would be limited by the necessity of extrapolating $\Delta G^{\ddagger}$ (ee → ae) to a higher temperature, but since it is known from NMR work that $\Delta S^{\ddagger}$ for nitrogen inversions is positive and not very large, the errors thus introduced would be small. The second scan technique, then, in principle provides a method for measurement of an equilibrium constant for which the minor component is not present in detectable concentration. To see experimentally if the technique would work, we first examined second scan data for **6,** for which K_{eq} is fairly small, but measurable by NMR and first scan CV. Second scan data were collected at −17 and −25 °C, giving kinetic parameters of 0.60 and 0.27, respectively. These kinetic parameters appear in the plot of Figure 3 as filled symbols, where it may be seen that they are noticeably high (the ratios of the second scan $K_{eq}\sqrt{k_t}$ values to those expected from the first scan data were 1.8 and 2.2, respectively). Compound **7** gives an opportunity to test the second scan technique on a compound for which K_{eq} has not been directly measured because it is too small, but was estimated from first scan data (see above). Unfortunately, there are serious difficulties involved in obtaining second scan data for such a case, because very low temperatures and fast scan rates must be used to observe an Hee wave on the second scan. Under these conditions the Hae wave has moved to such high potentials that it seriously overlaps with the second oxidation wave. Using data taken at −52 °C, 20 V/s scan rate, a value of k(ee → ae) of 102 s^{-1}, corresponding to $\Delta G^{\ddagger}$ (ee → ae) of 10.8 kcal/mol, was found. This $\Delta G^{\ddagger}$ is unacceptably low, and would require that either $\Delta G°$ is unreasonably negative, or $\Delta G^{\ddagger}$ (ae → ee) is unaccountably low compared to analogous compounds ($\Delta G^{\ddagger}$ (ee → ae) was estimated to be 12.5 ± 0.5 kcal/mol from the first scan data at 24 °C).

We suggest that some reasons for the high kinetic parameters and k(ee → ae) rates, which experimentally get worse as the temperature is lowered, are clear. Because the Hae wave overlaps with the second oxidation wave (and this overlap be-

Table VI. Estimated Shifts (ppm) for **13**e(ee) Compared with Observed Shifts for Species A

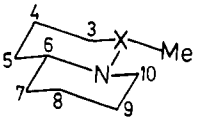

Carbon	X = CH[a]	Δδ(X = N) replacing X = CH)[b]	Estd for e(ee)	Obsd Sp. A	Δδ[c]
3	35.45	+23.21	58.66	58.63	−0.03
4	24.75	+0.03	24.78	24.69	−0.09
5	34.16	−1.15	33.01	33.01	0
6	63.23	+0.58	63.79	63.72	−0.07
7	33.97		33.97	33.86	−0.11
8	24.62		24.62	25.18	+0.56
9	26.39		26.39	26.59 (or 26.51)	+0.20 (or 0.12)
10	51.90	(+0.58)	52.48	52.57	+0.09
Me	20.78	+23.51	44.29	44.44	+0.15

[a] From ref 7. [b] Using shifts for 1,2-dimethylpiperidine and 1,2-dimethylhexahydropyridazine.[7] [c] Average deviation 0.14 ppm.

comes worse as the temperature is lowered in going from **6** to **7**), there is too much observed current for this wave, making our calculation of the expected Hee current too large. Furthermore, the second oxidation destroys $H^{+}\cdot$, so its reduction wave is smaller than it should be, also making less Hee be generated than we calculate. An additional factor is that destruction of $H^{+}\cdot$ releases protons which protonate hydrazine, keeping it from being oxidized as it diffuses in, further reducing the size of the observed Hee wave. All of these factors (and possibly others not mentioned) combine to make the Hee wave observed considerably smaller than our calculation says it should be for a given $k(\text{ee} \rightarrow \text{ae})$, resulting in the simulated rate being far too large. Although we could modify the simulation program to include the factors mentioned, and this would obviously improve the $k(\text{ee} \rightarrow \text{ae})$ calculated, we do not feel that inventing two more adjustable parameters which cannot be accurately determined would really result in what one would call a quantitative measurement of $\Delta G^{\ddagger}(\text{ee} \rightarrow \text{ae})$. Since we know that the rate constant for electron transfer from Hae is rather sensitive to experimental conditions,[1] we are currently attempting to find the proper conditions to get the Hae wave cathodic of the second oxidation wave and avoid the experimental problems; we have not yet had success.

Conclusions

K_{eq} for the ee,ae equilibrium of hexahydropyridazine derivatives can be directly measured by CV when the activation barrier separating the two is above about 11 kcal/mol. The CV numbers are slightly lower than those measured by NMR, probably owing to problems of overlap of the Hae oxidation wave with the second oxidation wave ($H^{+}\cdot \rightarrow H^{2+}$), although the differences are rather slight except when K_{eq} is large (and the Hae wave therefore small). Rate constants by NMR and CV agreeing to within a factor of about 3 were measured for some cases. Because the NMR and CV techniques differ significantly in the processes actually observed, in some cases they measure entirely different conformational processes, and combination of NMR and CV results can lead to new information, such as the estimates of K_{eq} for **7** and **14**, where NMR cannot detect the Hee form. Although analysis of the second oxidation scan will in principle allow direct measurement of rates inaccessible by NMR ($k(\text{ee} \rightarrow \text{ae})$ when no Hee is detectable), experimental difficulties presently preclude its quantitative application.

Experimental Section

3-Oxo-1,2-diazabicyclo[4.4.0]decane. A modification of its preparation by Mikhlina and co-workers,[12] who pyrolyzed the zinc reduction product of the *N*-nitroso acid, was employed. A mixture of 2.0 g of ethyl 3-(2-nitrosopiperidyl)propionate (yellow oil, prepared by standard methods from 3-(2-pyridine)acrylic acid[13]), 0.31 g of $FeSO_4 \cdot 7H_2O$, 1.5 g of 5% Pd on calcium carbonate, and 300 mL of water was hydrogenated in a Parr apparatus at 45 psig initial pressure. Ring closure occurred spontaneously, giving 1.29 g (90%) of the bicyclic hydrazide, mp 149–150 °C (lit.[12] 149–151 °C).

2-Methyl-1,2-diazabicyclo[4.4.0]decane (15) was prepared from the 3-oxo compound using $LiAlH_4$ reduction (benzene–ether) followed by sodium cyanoborohydride–formaldehyde reductive methylation[14] in 44% overall yield. **15** is an oil, purified by VPC. ^{1}H NMR (acetone-d_6) δ 1.1–1.8 (m, 10 H), 2.37 (s, 3 H), 2.39–3.15 (m, 5 H); empirical formula established by high-resolution mass spectroscopy. Table VI contains details of the estimated and observed shifts for the ^{13}C NMR spectrum of **15**e(ee).

Cyclic Voltammetry. The cell, electrode preparation, temperature control, and solvent purification techniques have been previously described.[1b] The instrument used was assembled from a PAR173 potentiostat, PAR179 coulometer, PAR175 Universal Programmer, Houston 2000XY recorder, and Tektronix 5000 series storage oscilloscope.

Table VII. E° Data for Tetraalkylhydrazines[a]

Compd	E°	Solvent
5	0.32	CH_3CN
6	0.31	CH_3CN
7	0.28	CH_3CN
8	0.39	$CH_3(CH_2)_2CN$
9	0.23	CH_3CN
10	0.31	CH_3CN
11	0.38	Acetone
12	0.40	Acetone
15	0.41	Acetone

[a] $(E_p^{ox} + E_p^{red})/2$ vs. SCE, 0.1 M tetra-*n*-butylammonium perchlorate, 100 mV/s scan rate.

Compensation of the effects of solution resistance was accomplished in the usual way.[15] The positive feedback compensation circuit was adjusted until incipient potentiostat oscillation but the adequacy of this procedure could not be fully evaluated because no highly reversible electrode reaction was available as a test system at low temperatures. Nevertheless, it was found that the above procedure for resistance compensation produced voltammograms with a peak separation of 65 mV (theoretical 47 mV) for oxidation of 2 mM 1,2-diazabicyclo[4.3.0]non-3-ene (which is exclusively in the rapid electron transferring Hee conformation) at the gold disk electrode in acetonitrile, 0.1 M tetrabutylammonium perchlorate, 0.200 V/s, −26 °C.

The standard oxidation potentials for the compounds employed are of no importance in the conformational analyses described in this paper, but the values measured in this work appear in Table VII. (These values and all other E° values mentioned in this paper are formal potentials corresponding to the supporting electrolyte concentration employed.) Differences between the compounds are not very great.

Digital Simulations. When K_{eq} is small (<0.5), the heterogeneous equivalent approach could be employed for the simulation program, as previously described.[1b] When K_{eq} is not small, one of the assumptions of the heterogeneous equivalent approach[16] is not valid, and we employed normal digital simulation techniques,[17] which did not consume inordinate amounts of computer time as long as the kinetic parameter, $K_{eq}\sqrt{k_t}$, was not too large (large Hee peak, tiny Hae peak, when K_{eq} is small). All simulations were performed using a Raytheon 706 computer. Our computer programs are available upon request.

Simulated curves were plotted at the same scale as the experimental curves, and compared visually using a light box. Several comparisons of the fits achieved appear in the Thesis of E. L. Clennan (University of Wisconsin, 1977).

References and Notes

(1) (a) S. F. Nelsen, L. Echegoyan, and D. H. Evans, *J. Am. Chem. Soc.*, **97**, 3530 (1975); (b) S. F. Nelsen, L. Echegoyan, E. L. Clennan, D. H. Evans, and D. A. Corrigan, *ibid.*, **99**, 1130 (1977); (c) D. H. Evans and S. F. Nelsen in "Characterization of Solutes in Non-aqueous Solvents", G. Mamantov, Ed., Plenum Press, New York, N.Y., 1977.
(2) R. P. Van Duyne and C. N. Reilley, *Anal. Chem.*, **44**, 142 (1972).
(3) (a) S. F. Nelsen and G. R. Weisman, *J. Am. Chem. Soc.*, **98**, 3281 (1976); (b) *ibid.*, **98**, 7007 (1976).
(4) S. F. Nelsen and E. L. Clennan, *J. Am. Chem. Soc.*, accompanying paper in this issue.
(5) S. F. Nelsen, *Acc. Chem. Res.*, 11, 14 (1978).
(6) Reference 3a; G. R. Weisman, Thesis, University of Wisconsin, 1976, p 53.
(7) R. J. LaLonde and T. N. Donivito, *Can. J. Chem.*, **52**, 3778 (1974).
(8) D. K. Dalling, D. M. Grant, and E. G. Paul, *J. Am. Chem. Soc.*, **95**, 3718 (1973).
(9) N. L. Allinger and J. L. Coke, *J. Am. Chem. Soc.*, **81**, 4068 (1959).
(10) F. W. Vielhapper and E. L. Eliel, *J. Org. Chem.*, **42**, 51 (1977).
(11) These estimations may be examined in the Thesis of E. L. Clennan, University of Wisconsin, 1977.
(12) E. E. Mikhlina, N. A. Komarova, and M. V. Rubtsov, *Khim. Geterotsikl. Soedin., Akad. Novk. Lativ, SSSR*, 91 (1966).
(13) W. Ried and H. Keller, *Chem. Ber.*, **99**, 2578 (1956).
(14) S. F. Nelsen and G. R. Weisman, *Tetrahedron Lett.*, 2321 (1973).
(15) P. E. Whitson, H. W. VandenBorn, and D. H. Evans, *Anal. Chem.*, **45**, 1298 (1973).
(16) I. Ruzic and S. Feldberg, *J. Electroanal. Chem.*, **50**, 153 (1974).
(17) S. W. Feldberg in "Electroanalytical Chemistry", Vol. 3, Marcel Dekker, New York, N.Y., 1969, pp 199–296.